Renewable and Sustainable Energy Reviews 20 (2013) 595–610

Contents lists available at SciVerse ScienceDirect

Renewable and Sustainable Energy Reviews

journal homepage: www.elsevier.com/locate/rser

Opportunities and challenges in micro- and nano-technologies for concentrating photovoltaic cooling: A review

Leonardo Micheli [a,*], Nabin Sarmah [a], Xichun Luo [a], K.S. Reddy [b], Tapas K Mallick [a]

[a] School of Engineering and Physical Sciences, Heriot-Watt University, Edinburgh, EH14 4AS, United Kingdom
[b] Heat Transfer and Thermal Power Laboratory, Department of Mechanical Engineering, Indian Institute of Technology Madras, Chennai 600 036, India

ARTICLE INFO

Article history:
Received 12 April 2012
Received in revised form
10 November 2012
Accepted 19 November 2012
Available online 23 January 2013

Keywords:
CPV
Passive cooling
Micro–nano-manufacturing
Monolithic

ABSTRACT

Concentrating photovoltaic technology is one of the fastest growing solar energy technologies achieving electrical conversion efficiency in excess of 43%. The operating temperature of a solar cell strongly influences the performance of a photovoltaic system reducing its efficiency with a negative temperature coefficient. Thus, cooling systems represent a very important aspect in concentrating photovoltaic applications. This work presents an overview of micro- and nano-technologies applicable to passive CPV cooling and associated manufacturing technologies (such as monolithic applications). Among the different technologies, carbon nano-tubes and high-conductive coating are the most promising technologies to offer the best CPV cooling performance. A critical assessment of the technological review has also been made.

Contents

* Corresponding author. Tel.: +44 131 451 4359; fax: +44 131 451 3129
E-mail addresses: lm298@hw.ac.uk (L. Micheli), ns158@hw.ac.uk (N. Sarmah), x.luo@hw.ac.uk (X. Luo), ksreddy@iitm.ac.in (K.S. Reddy), T.Mallick@hw.ac.uk (T. Mallick).

1364-0321/$ - see front matter
http://dx.doi.org/10.1016/j.rser.2012.11.051

1. Introduction

Up to now photovoltaic (PV) energy is still one of the most expensive energy source among both renewable and conventional sources. One promising approach to decrease PV costs is to reduce the amount of semiconductor materials needed. Some companies are manufacturing solar cell with thin silicon wafer to reduce costs [1]. Others use lenses or mirrors to concentrate sunlight onto cells: the replacement of semiconductor area with cheaper concentrating mirrors or lenses is a way to lower the cost of solar electricity. This solution is called *Concentrating Photovoltaic* (CPV).

Only a fraction of incoming sunlight striking any photovoltaic cell is converted into electrical energy. The rest of the absorbed energy converts into thermal energy within the cell [2]. At the end of 2011 the highest efficiencies of silicon single-junction cells [3] and for multi-junction cells [4] for one sun and AM1.5g spectrum were reported to be 25% and 34.1% respectively. While using with concentrating sunlight, increases in record efficiencies were reported which are 27.6% (AM1.5d, 92 suns) for Si cells [5] and 43.5% (AM1.5d, 418 suns) for multijunction cells [6]. Thus, a large amount of solar energy cannot be converted into electricity yet and is dissipated as heat.

The efficiency of any photovoltaic cell decreases with increasing temperature which is non-uniformly distributed across the cell. Martinelli and Stefancich [7] stated that "this fact can be viewed as a consequence of the second principle of thermodynamics imposing a limit on the conversion efficiency of energy coming from a source at a given temperature by a converter/sink having a finite temperature". Study has also shown that high temperature can cause long term degradation to the cell [8]. The rising temperature will also result in mechanical impact on the cell such as deformation on the cell surface, delamination of the transparent layer and development of micro-cracks on the cell. This is due to different thermal expansion coefficients of several different materials used to compose the cell structure. The temperature variation and, as a consequence, the different thermal expansion coefficients can lead to immediate failure in fragile components or to fatigue failure of the cell. This paper will review the state-of-the-art of the passive cooling systems that have been designed to overcome the thermal expansion and maintain the operating temperatures for concentrating photovoltaic systems.

2. Concentrating photovoltaic cooling

Cooling usually is not required in common flat PV systems and in the CPV systems with low concentration ratio ($CR \leq 5$); this is because of the large module surface and terrestrial energy flux of the sunlight. On the contrary, cooling is a real important aspect in medium and high concentrating CPV systems ($10\times < CR < 100\times$ and $CR > 100\times$ respectively), due to the significant reduction of the receiver surface and increase in the energy flux of the concentrated sunlight. Furthermore triple junction cells are particularly sensitive to temperature: the conversion efficiency of a three-junction cell can decrease 0.05% for every °C increase of cell temperature [9]. Taking into account a standard AM 1.5d solar insulation of 850 W/m^2 on a 500× CPV system, optical losses of 20% and a cell efficiency of 30%, a heat power of 23.8 W/cm^2 must be dissipated by the cooling system. Several common cooling technologies, including fins, micro-channels and heat pipes, can be applied to the CPV systems, as reported by Royne et al. [2]

2.1. Passive cooling

Usually cooling systems are classified as *passive cooling* and *active cooling* depending on the cooling mechanism. Passive cooling does not require input of mechanical or electrical power as it acts through the exploitation of natural laws, whereas active cooling requires external energy to cool the solar cells.

Earlier review articles on cooling system for the CPV system stated that passive cooling was not feasible for any densely packed cells or for linear concentrators with concentration ratios above 20 suns [2]. There were very few passive cooling techniques available in the market as reported by Yeom and Shannon [10]. While reviewing micro-cooler, Yeom and Shannon discussed only a few passive cooling technologies for the CPV system.

Some theoretical researches have been published with the aim to investigate the opportunities of a passive approach for electronics cooling. In 2007, Tseng et al. [11] applied Taguchi's statistical method to optimise the passive cooling systems for electronic devices. According to the authors, application of Taguchi's method will contribute to the reduction of manufacturing costs of the electronic device. They demonstrated that openings in the mother board, power density and flow pattern are the most important parameters to determine the device's thermal behaviour. Furthermore, they stated that passive cooling is more reliable and even better than the inclusion of forced flow, and can reduce the damage probability caused by the cooling failures.

2.2. Active cooling

Active cooling is obtained using a fraction of the cell power output. Thus, a part of the energy output would not be available for further use. But active cooling is independent of the work conditions and is usually easily controllable than passive cooling. Micro-channels heat sink or impinging jets seemed to be the most promising technologies for active cooling of a CPV plant as reported by Royne et al. [2].

In 2009 Zhangbo et al. [8] presented new definitions for passive and active cooling. In their definition, active cooling referred only to the so-called photovoltaic/thermal collector (PV/T) technology: the heat produced by the PV is removed from the cell and it is re-used in other applications. This new "active cooling" concept does not include necessarily micro-channels or fluid jets impingement.

Table 1
Comparison of convectional nanofabrication techniques [27].

Technique	*Resolution*	*Throughput (wafers/h)*	*Cost*	*Application*
Contact lithography	˜λ	< 10	$	R&D
Proximity lithography	˜3 μm	< 10	$	R&D
Projection lithography	32 μm	> 100	$$$	Industry
Extreme Ultraviolet lithography	22 μm	˜10	$$$	Industry

2.3. Target of CPV cooling

During the CPV cooling system design, several parameters must be considered, such as the local direct normal insulation, the system geometry and the concentration ratio. The requirement for cell cooling mainly depends on the CPV system's geometry. A densely packed cell assembly represents the most difficult configuration to be cooled. In that case a thermal resistance of less than 10^{-4} m^{2}K/W is required under any concentration above 150 suns [2].

2.4. State-of-the-art of CPV cooling

Fins or heat spreaders are generally used in low concentrating systems. In 2008, heat pipes have been successfully tested for CPV passive cooling [12]. Several different technologies have been applied for high CPV cooling. As already mentioned, active liquid cooling is usually employed for densely-packed systems with high concentration. In particular, during the last years, several investigations were reported on liquid immersed solar cells [13–16]. This is an active cooling solution: solar cells are immersed in a circulating dielectric liquid. According to Zhu et al. [16], the convective heat transfer coefficient could be higher than 3000 W/m2K for concentrations higher than 200 suns.

Mokri and Emziane [17] reported installation costs as low as 3.05 $/W and levelized cost of energy (LCOE) as low as 0.14 $/kWh for CPV with high concentrations in 2010. Gombert [18] reported that the material choice has a great impact on the cost of CPV. The assembly represents 20% of the cost of the whole CPV system, which includes the cooling system [19]. This shows that the prices of cooling system materials and manufacturing strongly influence the cost of the system and actively take part in the economic competiveness of the CPV in the energy market.

3. Micro- and nano-technologies for cooling CPV system

The development of micro- and nano-technologies offers new perspective for CPV cooling. Small dimensions and high demonstrated performances of micro- and nano-technologies will play an important role for CPV coolers.

3.1. Principles

Since the concentration of sunlight leads to a reduction of the irradiated surface, mesoscale cooling device may not be appropriate to remove great amount of heat from small surfaces. On the other hand, when the size drops below 100 nm, important changes in material properties can occur. Additionally, according to Shakouri [20], in the nano-meter domain there are new unique effects due to quantum phenomena and enhanced surface to volume ratios. Bhushan [21] defined nano-technologies as "any technology on a nano-scale that has application in the real world". Micro- and nano-technologies can assure faster performance, requiring both less space and less material than common devices. A lot of researches have been focused on micro- and nano-cooling technologies, due to their importances in electronics: micro- and nano-scale electronic devices can generate heat fluxes exceeding thousands watt per centimetre square [20].

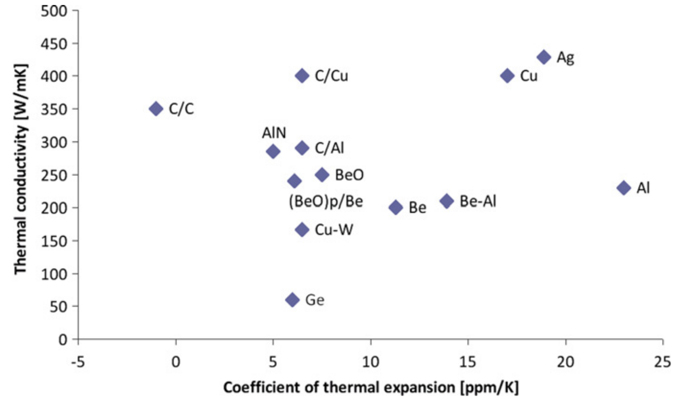


Fig. 1. Thermal conductivities vs. CTEs. Thermal conductivities vs. coefficient of thermal expansions of different materials.

3.2. Efficiencies

Royne et al. [2] defined the micro-channels heat sinks the best performing cooling systems for a high concentrating photovoltaic system. In 2011, Müller et al. [22] investigated the micro-channels performances in a 1500× CPV. They showed that the system remained fully functional up to 4930 suns and registered a decrease of 1% in the photovoltaic efficiency for every 100 suns concentration increase. In their review, Yeom and Shannon [10] reported that micro-coolers were able to remove heat flux up to the value of 500 W/cm^2.

3.3. Micro- and nano-cooling technologies

As underlined by Gururatana [23], since the industry is moving towards micro-scale electronic products (such as laptops and smart phones) to meet the specifications for portable design, dissipated heat from micro-scale electronic components become a serious issue. Several papers were published on micro-cooling, but none is strictly focusing on the passive micro-cooling and its application to the CPV systems. In 1998 Gromoll [24] reported a review of micro-cooling systems based on forced air cooling for high-density electronic components packaging. Nano-scale thermal transport advances were reported in 2003 by Cahill et al. [25] and by Shakouri in 2006 [20].

3.4. Micro- and nano-cooling manufacturing

The nanotechnology manufacturing techniques can be divided into conventional and unconventional processes. The first ones, such as photolithography and electron beam lithography, use light or electrons to generate patterns. Conventional techniques are the most widely used techniques. According to Gates et al. [26], the cost of purchasing, installing, and maintaining the tools they require limits their application in areas other than microelectronics. A summary of the convectional nanofabrication techniques are given in Table 1. The others, those reminiscent of macroscopic molding, embossing, printing and skiving technologies, are indicated as the ultimate, low cost solutions [27]. They are usually developed to overtake the technical or financial limitations of conventional methods.

Table 2
Costs comparison among copper, diamond/copper composites and diamond.

Copper	Cu/D composites	Diamond
~400 W/m^2	800–1200 W/m^2	1000–1800 W/m^2
\$0.06 per cm^3	\$1–10 per cm^3	\$3000 and \$6000 per mm^3

4. Coolers

A list of micro- and nano-technologies for cooling electronic devices has been reported. The cooling technologies described in this review should be summarised in the following ways:

- Air cooling: heat spreaders, natural convection in micro-channels, carbon nano-tubes, micro-fins, nano-wires (not intended as thermoelectric devices).
- Liquid cooling: natural convection of nano-fluids, micro-heat pipes, miniature thermosyphons.

4.1. Heat spreaders

The heat spreader consists of a layer of high thermally conductive material which allows removing the heat from the cell. It can be used in junction with a heat sink. Jagannadham et al. [28] reported a list of important necessary characteristic features for heat spreaders: high thermal conductivity, high dielectric constant and high specific heat. Abyzov et al. [29] added few more features, such as a coefficient of thermal expansion (CTE) close to those characteristic for semiconductors (silicon or germanium in this case), stability under thermal cycling in the operating temperature, low specific height, manufacturability and low cost.

According to Bar-cohen and Wang [30], due to the high thermal conductivity of silicon (~150 W/mK), only modest spreading improvements can be obtained from the use of traditional spreading materials, such as copper (390 W/mK), beryllia (250 W/mK), aluminium nitride (220 W/mK). Furthermore, beryllium oxide, traditionally used as a heat spreader, is expensive and toxic. Aluminium and copper are good heat conductors, but their coefficient of thermal expansion is higher than that of germanium or silicon. Composite materials such as Cu–W or Al–SiC are less expensive, however the thermal conduction is usually lower than 250 W/mK. No common composite materials show thermal conductivity higher than 400 W/m2, (Fig. 1). Higher thermal conductions can be obtained with pyrographite and diamond composites. Pyrographites plates are strongly anisotropic and thus cannot be easily applied [29]. Carbon nanotubes have been considered for composite materials, due to their high conductivity. Unfortunately, while showing important enhancements in mechanical properties, CNT composites cannot be considered as a promising option yet [29].

Diamond is indicated as a very good material for electronic heat spreading [28,30,31], due to its extremely high thermal conductivity (500–2100 W/mK, the highest values among all the known materials) and its very high electrical resistance (~10^{18} Ωm). Bar-cohen and Wang [30] defined the deposition of diamond on substrates such as silicon, as a "reasonably mature technology", able to assure good results. This was also confirmed by Zhang et al. [32] and Twitchen et al. [33], who stated that the thermal conductivity of the best quality synthetic diamond grown by Chemical Vapor Deposition (CVD) is identical to that of high purity natural type diamond at room temperature (2200 W/mK). After having proved its matureness and the high quality of its deposition method, the deposition of a diamond layer on the receiver seems to be a good solution for CPV cooling.

Jagannadham et al. [28] noted that the low molar heat capacity of diamond makes it good for distribution of energy rather than dissipation. For this reason, they suggested that the low heat capacity of the diamond can be compensated through a higher heat capacity substrate on which the diamond is deposited. In their heat spreader design, the authors used an intermediate layer of aluminium nitride under a continuous layer of diamond. An increase in heat spreader characteristic and life time was observed compared to a single layer diamond and a bar molybdenum heat spreader. On the other hand, Zhang et al. [32], simulating in COMSOL the performances of a polycrystalline CVD diamond thermal substrate as a part of active cooling for power devices, observed that there is no improvement in cooling by replacing the aluminium nitride with diamond in a DBC, because of the higher value of the thermal convection resistance than that of the thermal conduction resistance. Once all the redundant layers were removed, they demonstrated an increase in the power dissipation of the systems by two times by replacing the ceramic with the diamond. A further increase in performances was then obtained by depositing a layer of copper micro-pillars onto the backside of the diamond substrate.

Diamond deposition is obviously an expensive process, which is the main limitation of this technology. The cost of the thermal diamond substrate can be within €1–10 per mm^3 as reported by Zhang et al. [32]. Recently Abyzov et al. reported the cost to be within \$3 and \$6 per mm^3 for CVD diamond plates with a thermal conductivity of 1000 and 1800 W/mK respectively [29]. So diamond composite is still an expensive option compared to copper (a 99.9 wt% purity copper plate costs about \$0.06 per cm^3) [29]. Sung et al. [34] had to face the high cost of the diamond film as well and obtained cheaper spreaders infiltrated with copper or aluminium

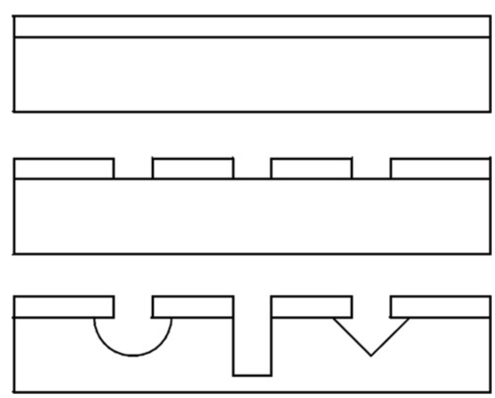


Fig. 2. Channel in silicon. Schematic of making a channel in silicon, adapted by [42].

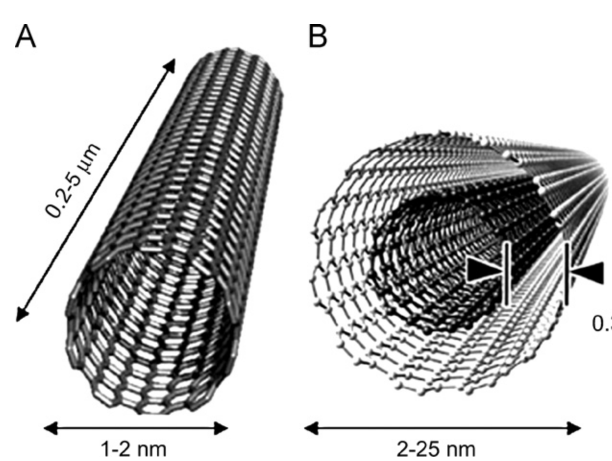


Fig. 3. SWNT and MWNT. Conceptual diagram of a SWCNT (A) and a MWCNT (B) [49].

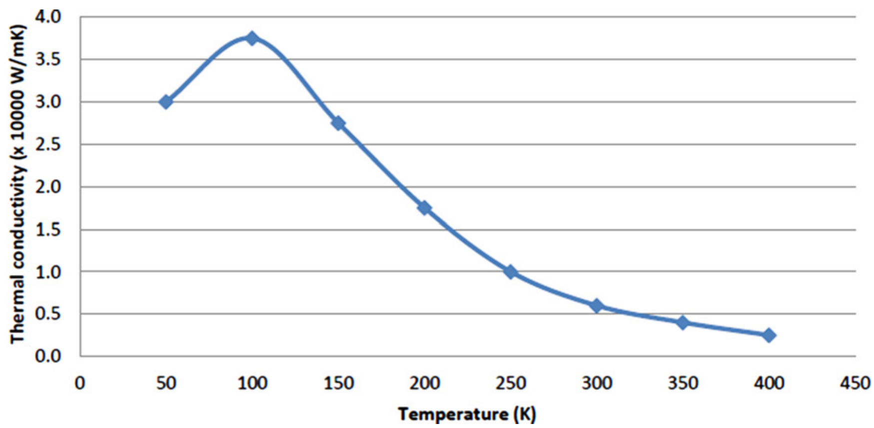


Fig. 4. CNTS's temperature dependence. Example of temperature dependence for a carbon nano-tube for temperatures below 400 K, adapted by Berber et al. [58].

with thermal conductivities respectively increased by factors of 2 and 1.5 times compared to the copper one. Composites of diamond particles can be a good compromise between costs and performances. The cost of diamond–copper composite material with a thermal conductivity between 800 and 1200 W/mK is less than 1/20 the cost of a CVD-diamond [29]. Reported analytical calculations estimated a price between \$1 and 10 per cm^3 for a copper material with 63% volume fraction of diamond particles. This estimation does not take into account the production costs, however it underlines the differences in costs among copper, diamond–copper composite and CPV–diamond (Table 2).

Cu/Dia is the most promising diamond composite, because of the low cost and high thermal performances of the copper. Composites with diamond filler and metal binder can be made by sintering or infiltration process. These operations can be run at ultrahigh pressures (> 1 GPa) or at a pressure between 1 and 100 MPa, depending on the materials [29]. Diamond composites' production process is really important, because the manufacturing process affects the thermal conductivity of the product [35]. In the worst case it can lead to a thermal conductivity of the composite lower than expected as reported by Nishiyabu et al. [35]. The diamond powder in air is thermally deteriorated at the conventional copper powder's sintering temperature: this means that diamond powders can be thermally damaged when sintered with copper powders. Furthermore, the presence of small-sized pores between copper and diamond powders can negatively affect the thermal conductivity. The authors concluded their work stating that further studies to improve thermal conductivity are necessary.

4.2. Natural convection in micro-channels

Micro-channels are composed of many parallel micro-cavities, with a hydraulic diameter ranging from 10 to 1000 nm. The forced convention in micro-channels contributed to achieve the best performance cooling which should be suitable to a high concentrating photovoltaic system [2]. Micro-channels have been substantially investigated for active cooling applications [2,10,36,37]. On the other hand, according to Buonomo and Manca [38], natural convective gas flows in micro-cavities, such as micro-channels, have not received much attention. More investigations are needed to understand the potentials of natural convention in micro-channels for CPV cooling.

In 2005 Chen and Weng [39] analytically investigated the natural convection in micro-channels and reported that the volume flow rate at micro-scale is higher than that at macroscale, while the heat transfer rate is lower. In an investigation on natural convection in vertical micro-channels, Buonomo and Manca [40] observed that the highest mass flow rate can be obtained at the highest Knudsen number (*Kn*) without significant changes in the average Nusselt number in terms of the heat flux ratio. In 2012 Buonomo and Manca [38] further investigated the natural convection in a vertical micro-channel. They showed that wall temperature profiles increased with increasing *Kn* and the differences between wall temperature profiles, for different *Kn* values, decreased with the increasing channel height. Furthermore, mass flow rate increased with increasing *Kn*, whereas Nusselt number decreases with increasing *Kn*. Haddad et al. [41] studied laminar free-convection flow in open-ended micro-channels filled with a porous medium. They found that heat transfer decreases with the increase of the Knudsen number and the thermal conductivity ratio.

4.2.1. Micro-channels fabrication

The fabrication approaches for micro-channels have been reported in several papers. In 1997 Tjerkstra et al. [42] listed four ways of fabrication of micro-channels by etching: wet anisotropic, wet isotropic, dry anisotropic and dry isotropic. The basic approach for constructing channels in silicon is depicted in Fig. 2. Silicon is covered with a mask material which was patterned and then etched. The channel on the left of Fig. 2 is etched isotropically, the middle anisotropically using Reactive Ion Etching (RIE), and the channel on the right is etched anisotropically in a KOH solution. Furthermore, Tjerkstra et al. [42] classified micro-channel machining methods into two groups: technologies involving bonding and not involving bonding.

Dwivedi et al. [43] in 2000 presented a new wet anisotropic method to fabricate long and deep micro-channels in silicon with smooth sidewalls. In their work, an etchant based on KOH, water and 2-propanol was used.

Dry etching can be obtained using laser micro-machining. Alavi et al. [44] used laser melting and anisotropic etching to fabricate micro-channels with high aspect ratio. Kam et al. [45] developed a flexible and fast femtosecond laser ablation of micro-channels in silicon to develop branching networks to serve as gas exchangers. Chen et al. [46] used this technique to produce 5 μm diameter micro-channels in a silicon substrate by femtosecond laser with 800 nm wavelength, which is in the absorption region of silicon.

4.3. Carbon nano-tubes

In 1991 Iijima [47] reported the synthesis "of a new type of finite carbon structure consisting of needle-like tubes" referred to as Carbon Nano-tubes (CNTs). Carbon nano-tubes are hollow cylinders made of graphite sheets. Their diameters and lengths

Table 3
Comparison of the established techniques for CNT synthesis, adapted by See and Harris [57].

Method	Arc discharge	Chemical vapor deposition	Laser ablation	High pressure carbon monoxide
Description	Arc evaporation of graphite in the presence of inert gas; CNT formed on electrodes, during quenching	Decomposition of hydrocarbons over transition metal catalyst to form CNT	Vaporisation of graphite target by laser; CNTs formed on receiver during quenching	Nucleation surface for the growing of CNT provided by the reaction of $Fe(C0)_2$ and CO
Operating temperature	$>3000\ ^{\circ}C$	$<1200\ ^{\circ}C$	$>3000\ ^{\circ}C$	$<1200\ ^{\circ}C$
Operating pressure	50–7600 Torr generally under vacuum	760–7600 Torr	200–750 Torr	7600 Torr
Advantages	Good quality CNTs	Easy scale up; synthesis on templates possible	Good quality CNTs; single conformation SWNT formed (10,10)	High-quality SWCNTs, run continuously
Disadvantages	Difficult to scale up	Quality of CNT not as good	Difficult to scale up; expensive	N.A.

are in the order of nm and μm, respectively. CNTs have high mechanical strength and good thermal conductivity. They are usually classified into two categories (Fig. 3), differing both in diameter and in thermal properties:

- *Single-walled carbon nano-tubes* (SWCNT or SWNT): individual cylinders 1–2 nm in diameter, consisting of a single rolled grapheme sheet. SWCNTs have important electric properties, but are still very expensive to produce [48].
- *Multi-walled carbon nano-tubes* (MWCNT or MWNT): nested graphene cylinders coaxially arranged around a central hollow core and held together by interlayer van der Waals forces. Diameters range from a few nm to hundreds of nm and the length can be as high as 100 nm.

Sometimes CNTs with only two layers are grouped in a category different from MWCNT and are called *Double-walled carbon nano-tubes* (DWCNT or DWNT) [50]. Depending on the change in properties, the CNT's are also categorised as *few-walled nanotube* (FWNT) and defined as a group of carbon-nanotubes composed of nanotubes with 2–5 layers of graphene shells on their sidewalls and generally with diameter smaller than 10 nm [51].

CNTs attracted significant attention due to their important thermal and mechanical properties, and several studies were carried on their applications in chip cooling. The potential uses of CNTs have been investigated in several fields, such as medicine [49], electronics, aerospace, field emission and lighting [52].

In 2010 Han and Fina [53] published a review of carbon nanotubes and their polymer nano-composites thermal conductivities. In 2010 Aqel et al. [48] published a wide review on carbon nanotubes. Shakouri [20] reports that upper bound for CNTs thermal conductance can be set at 4×10^9 W/m^{2}K at room temperature. An increase of 400% in the heat transfer coefficient was demonstrated by a group at Purdue, using CNT arrays on a chip surface [10]. In 2011 Chiavazzo and Asinari [54] investigated CNTs as alternatives in heat transfer to nano-fluids.

Kim et al. [55] measured the thermal conductivity of a single carbon nano-tube. They observed the value was around 3000 W/mK. But Jakubinek et al. [56] reported that "the heat dissipation ability of CNTs has not translated to bulk CNT materials". Tong et al. [57] determined a thermal conductivity of 250 W/mK for a MWCNT array, grown on Si wafer by thermal chemical vapour deposition (CVD) process with transition-metal iron (Fe) as catalyst. As reported by the authors, taking into account an estimated fill-in ratio of 10%, this result matched the experimental ones, obtained just for a single CNT.

Jakubinek et al. [56] used vertically aligned MWCNT arrays, grown by water-assisted CVD to investigate thermal and electrical conductivities of CNTs. Nano-tubes had a diameter of 10–20 nm and were spaced approximately every 70–100 nm. The authors measured a thermal conductivity in the range of 0.5–1.2 W m^{-1} K^{-1} at 300 K, with the shortest array having the highest values. Moreover, scaling the arrays' value, they determined the thermal conductivity of an individual MWCNT, which was in a range of 18–42 W/mK.

Berber et al. [58] carried out a simulation study in order to determine the CNTs thermal conductivity and its dependence on temperature. The results of their investigation are reported in Fig. 4. Combining equilibrium and nonequilibrium molecular dynamics simulations with accurate carbon potentials, the authors obtained a value of 6600 W/mK for an isolated nanotube at room temperature, which is higher than that of diamond. Their study suggests that at $T=100$ K, carbon nano-tubes show an unusually high thermal conductivity value of 37,000 W/mK. As reported by Han and Fina [53], this trend is in disagreement with the experimental result obtained by other works.

Kordas et al. [59] tested a 1.2 mm long laser patterned CNTs on a 1 mm^2 silicon chip. Tests took place with various thermal loads (up to 7 W) and cooling gas (N_2) flow rates. The authors discovered that the application of the nano-structure allows the dissipation of 30 and 100 W/cm^2 more power at 100 °C from a hot chip than in the cases of natural and forced convections, respectively. According to the reported data, CNTs are one of the most interesting solutions for CPV passive cooling, due to their high heat transfer properties.

4.3.1. CNTs manufacturing

There are four commonly used methods for synthesising CNTs: arc discharge, chemical vapour deposition, laser ablation and High Pressure Carbon Monoxide (HiPco) processes. The most important characteristics of these methods are reported in Table 3.

4.3.1.1. Arc discharge. CNTs self-assemble from carbon vapour created by an arc discharge between two carbon electrodes. Arc discharge method was used by Iijima [47] in the first CNTs synthesis. Keidar [69] stated that CNTs produced by the arc discharge technique have fewer structural defects than those produced by low temperature techniques, while this method produces large quantities of impure material [48]. Every year, hundreds of works are being published on CNTs growth by the arc discharge technique.

4.3.1.2. Chemical vapour deposition synthesis. Chemical Vapour Deposition (CVD) is the most commonly used method to produce CNTs. In this method CNTs are grown using catalysis, which involves decomposition of a hydrocarbon gas over a transition metal catalyst and the initiation of CNT synthesis by some of the resulting carbon atoms. CVD generally results in MWCNTs or poor quality SWNCTs [48]. The growth of individual single-walled carbon nano-tubes (SWNTs) by chemical vapour deposition has been tested on several elements [70,71].

4.3.1.3. Laser ablation. A high power laser beam impinges on a volume of carbon containing feedstock gas. The CNTs formed by the laser ablation method are of a higher quality than those produced by the arc discharge method. However, the production rate is low, and the pulsed laser vaporisation or laser ablation method is both capital and energy intensive [72]. In 2002 laser ablation techniques were reviewed by Maser et al. [73], who concluded that these methods were not compatible with large scale production. Furthermore, they added that a large potential in using different lasers and combination of lasers was still unexplored and that cheaper feedstock materials and more efficient processes were the milestones for a low cost production.

4.3.1.4. High Pressure Carbon Monoxide. High Pressure Carbon Monoxide process is a low-cost gas-phase catalytic process developed in 1999 at Rice University by Richard E. Smalley and his co-workers [74] to grow SWNTs. The basic principle of this method consist in the decomposition of $Fe(CO)_5$ in CO at high pressure and temperature. According to the authors, the HiPco process can run continuously. In some work it is reported as a CVD process ("via the decomposition of volatile metallo-organic compounds within the reactor, without the use of a substrate") [75]. Others authors reported it by itself [76].

4.3.1.5. Alternative processes. Apart from the above methods, other synthesis processes can be found in literature, such as plasma torch method [77–79] and electrolysis [80] to fabricate CNTs. Flame synthesis is one of the most extensively researched alternative methods [72,81–83].

Unfortunately, although the previous methods can produce large quantities of CNTs, the cost is generally still too high to make any large-scale applications. Continuous synthesis of CNTs allows growing large quantities of CNTs effortlessly. According to Ying et al. [50], who published a review of continuous synthesising methods in 2011, research in the continuous synthesising process has made some progress in both the arc method and the CVD method while other continuous methods are currently not generally known.

CNTs usually contain impurities, type and amount of which depend on the synthesis process. The most common impurities are carbonaceous materials. These impurities influence CNT properties and limit their applications. Several purification processes have been proposed, such as oxidation [84–86], acid treatments [87] and filtration [88]. Different techniques can be combined to improve purification [89].

Some groups investigated on high purity synthesis methods to avoid the purification processes, which usually cause changes in CNTs properties. In 2006 Hong et al. [90] proposed first a high purity CNTs production process. Through the catalytic decomposition of methane with NiO/TiO2 as a catalyst, they obtained MWNTs with 99.9 wt% purity. In 2007 Dasgupta et al. [91] proposed catalytic chemical vapour deposition of acetylene diluted with nitrogen. Cobalt formate supported on carbon black was used as the catalyst. The purity of the obtained nano-tubes was 96%. In 2012, a model to determine and compare the cost of the SWNT synthesised by arc discharge, CVD and HiPCo was developed by Isaacs et al. Their results show cost per gram of $1.906, $1.706 and $485 respectively. According to the authors, the HiPco method has the lowest cost because this method is able to re-circulate CO in a continuous process [76]. Fleury et al. [92] noted that the prices of CNT–polymer nanocomposite can even rise if safety costs for CNT–polymer nanocomposites production are considered, due to safe process design and workplace organisation, personal protective equipments and safety management during the maintenance procedures. Starting from the data exposed by Isaacs et al. [76], Ok et al. [93] estimate the costs for SWNT manufacturing using a Monte Carlo model they developed. The results confirm the cheapness of the HiPCo process, when compared to the arc discharge and CVD processes. They finally foresee the variation in prices due to a voluntary implementation of higher EHS standards by the industries.

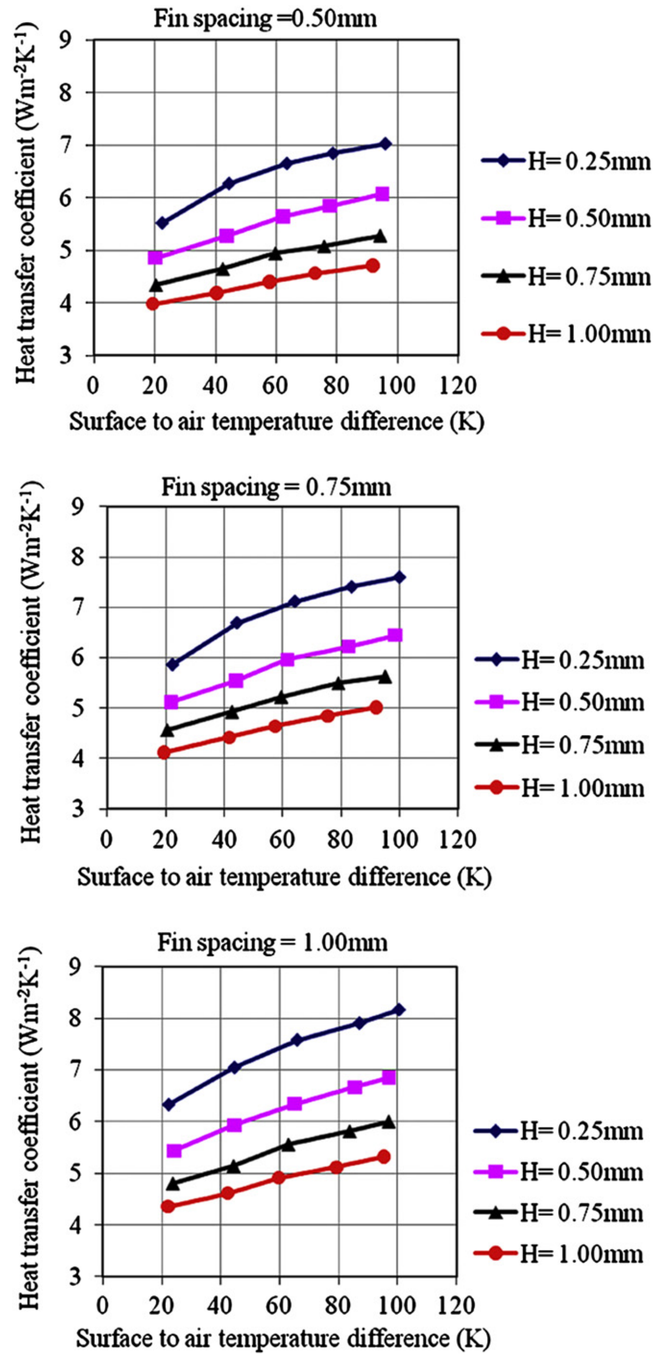


Fig. 5. Fin height vs. HTC. Effect of fin height on the heat transfer coefficient [98].

4.4. Micro-fins

Heat transfer around macro-fin arrays has been extensively researched. They allow increasing the heat transfer, through the extension of the exchanging surface. Macrofins are widely used, from the radiators to the printed circuit boards. They have been used for CPV cooling too. Natarajan et al. [94] investigated the use of cooling fins in a Low Concentrating Photovoltaic plant. They

concluded that the thickness and the thermal conductivity of the back plate of the receiver are important in reducing solar cell temperature. The lowest solar cell temperature is obtained when the back plate is made of a high conductive material such as copper. Compared to the worst case, the best configuration allows a reduction of 35% in cell temperature. In 2012, Do et al. [95] demonstrated that the total heat loss by convection and radiation from a CPV heat sink is 24–26% of the total input power.

Attaching fins to the base of the backplate, Natarajan et al. [94] analysed the influence of fin number in cell cooling. The authors defined a maximum number of fins that appear to be effectively convenient in the case considered. Moreover, they reported that the thickness of fins does not significantly change the cell temperature: "use of larger fin thickness increases the conduction heat loss, but at the same time suppresses the convection heat loss in between the fins". Fin length influences the cell temperature too, but material and cost reasons do not allow increasing it too much. A co-relation between the fin spacing, the inclination angle and the temperature difference for a CPV setup cooled by a plate-fin heat sink has been developed and reported by Do et al. [95] after a detailed investigation on the relationship between the thermal resistance, inclination angle and the input power. However these conclusions are in disagreement with the previous work of Mittelman et al. [96], who stated that "the optimal fin spacing of tilted arrays is almost identical to that of horizontal arrays". Study reveals that a detailed study on the fin structure and the spacing is necessary for individual CPV system designed to operate with different solar cell temperatures.

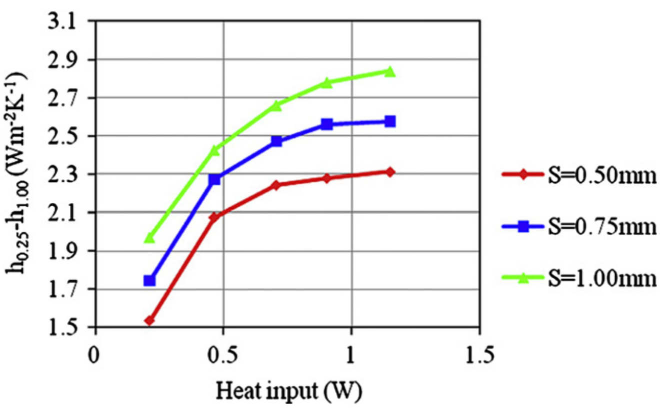


Fig. 6. Fin spacing vs. HTC. Effect of fin spacing on the heat transfer coefficient [98].

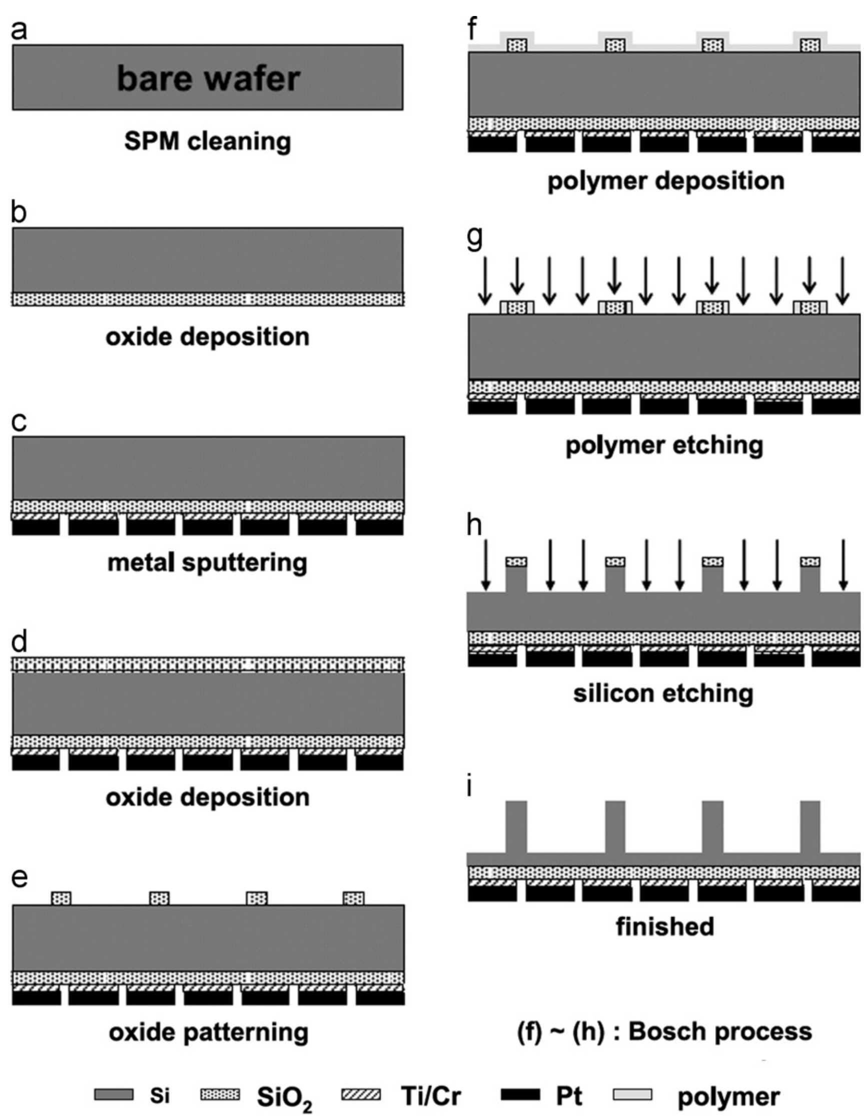


Fig. 7. Micro-fins machining. Fabrication procedure of Kim et al. [97] micro-fin arrays.

Although lot of papers focused on cooling macro-fins, only a few researches on micro-fins arrays [97–99] were reported. Kim et al. [97] demonstrated that the heat transfer correlation for macrofin arrays is inadequate for the accurate estimation of the heat transfer rate in micro-scale systems. Moreover, they added that the orientation effect is negligible at micro-scales.

Mahmoud et al. [98] carried out an experiment to investigate the effects of micro-fin geometry on natural convection heat transfer of horizontal micro-structures. They discovered that the values of convective heat transfer coefficient increased with decreased fin height (as shown in Fig. 5) or with increased fin spacing (Fig. 6). Among the several tested layouts, the highest value for convective heat transfer coefficient of 8 $Wm^{-2}K^{-1}$ was recorded at the lowest fin height of 0.25 mm and spacing of 1.0 mm.

Shokouhmand et al. [99] conducted a numerical investigation on natural convection and radiation heat transfer from micro-fin array heat sinks. They discovered that radiation exchange contributes up to 22% of the total heat dissipation, thus it should be included in the study of natural convection micro-fin heat sinks.

Micro-fins are a simple solution to improve the cooling of the system, even if their performances seem to be lower than CNTs ones.

4.4.1. Micro-fins fabrication

Micro-fins can be obtained through standard wet or dry etching process. Mahmoud et al. [98] used a micro-electro discharge wire machining (m-EDWM) process to fabricate their prototypes. Kim et al. [97] fabricated micro-fin arrays with fin heights of 100 and 200 μm in a bulk silicon wafer using Microelectromechanical systems (MEMS) process. The procedure was divided into two major steps: the metal deposition process for the electric heater, and the deep etching process for fin geometries. The second step was realized through Deep Reactive Ion Etching (DRIE, from (*f*) to (*h*) in Fig. 7). DRIE is a widely used process for deep trench etching of a silicon wafer. The most common DRIE technique is the Bosch process, patented by Robert Bosch GmbH in 1994 [100] and based on alternating multiple steps of etching and sidewall passivation. Even Peles et al. [101] used DRIE process to evaluate the forced convective heat transfer across a bank of micro-fins. In 2009 Bopp et al. [102] presented a new DRIE process to obtain different micro- and nano-structures, i.e. fins and nano-wires, arranged on two or more levels in bulk silicon.

Dry etching techniques, also known as Reactive Ion Etching (RIE), are processes that combine physical and chemicals effects to remove material from the wafer surface [103]. Wet etching should be faster than dry etching, but has some disadvantages, which were reported by Murakami et al. [104]. Required structures cannot always be fabricated by the wet etching process because the etched geometry by the etchant depends on the crystalline orientation. In addition, micro-structures are often stuck together during dry up after the wet procedure because of the surface tension force of liquid. On the other hand, the authors stated that dry etching procedure can solve these problems. A cryogenic RIE process was finally demonstrated to fabricate 3-dimensional silicon micro-structures with a high aspect ratio. According to Laermer et al. [103], the most important feature of RIE, compared to wet etching, is the capability of directional (anisotropic) etching without relying on crystal planes of the material. DRIE is considered an extension of the RIE and grants higher-rate etching of deep and narrow structures. Furthermore, DRIE usually allows better selectivity and process controllability than RIE. Kosar et al. [105] used RIE process to remove oxide in wafer places not protected by the resist and then DRIE process to etch silicon and to fabricate their low aspect ratio micro-pin fins.

In 2008, Abdolvand and Ayazi [106] developed a new DRIE method, modifying the Bosch process. Adding an argon/oxygen plasma pulse between the passivation and etching steps and a short oxygen clean step at the end of each cycle, the authors obtained very high aspect-ratio sub-micron trenches in silicon.

4.5. Nano-wires

A nano-wire is a one-dimensional nano-structure: its length is much more extended than its diameter, which is constrained to tens of nano-metres. According to Zhang [107], in the last decade nano-wires have been applied in several fields, such as biosensors and electronic devices. In addition, in 2009, Li et al. [108] designed a PV module made of periodic Si nano-wire arrays. The authors found that silicon nano-wire arrays can reach the same superior ultimate efficiency than the Si film with the same thickness.

Nano-wires are usually used as thermoelectric devices [109], due to the high electrical conductivity and low thermal conductivity [110,111]. They directly convert heat into electricity. Due to their low thermal conductivity they are not suitable for passive cooling.

4.6. Natural convection of nano-fluids

One of the most important problems in the development of energy-efficient heat transfer systems is the low thermal conductivity of fluids. In 1993, Masuda et al. [112] firstly investigated the thermal conductivity of water containing Al_2O_3 nanoparticles, reporting an enhancement in thermal conductivity. Choi and Eastman [113] proposed the concept of nano-fluids in 1995, in order to improve the thermal conductivity of fluids. They carried out a theoretical study to foresee the benefits of copper nano-particles suspended in water. Nano-fluids are fluids with nano-particles suspended in them. Nano-particles have at least one of their principal dimensions smaller than 100 nm. The choice of nano-particle in nano-fluids can be crucial to achieve good thermal properties. The following criteria reported by Rafati et al. [114] can be the benchmark to choose nano-particles for different applications:

- High stability in selected base fluid and lower tendency to agglomeration and settling.
- High hermal performance in suspension even at low concentration.
- Availability and reasonable price.
- Non-toxic and environmental friendly.

Nano-fluids find application in several fields, from biomedical to heat transfer applications [115]. In 2010 Godson et al. [116] presented a review about nano-fluids. A section of their work is dedicated to the natural convection experiments. It was reported that only limited experimental studies and contradictory results were available and, thus, further investigations were necessary on this subject [117]. The few reported experimental data and measurement methods also underlined the inconsistency in results [118]. Significant discrepancies among the characteristics measurements (i.e. thermal conductivity and viscosity) for any nano-fluids application have been reported which are possibly due to the lack of standard for nano-fluid preparation, different sources of nanoparticle manufacturing, various stabilisation methods and time duration between the preparation and the measurement.

Ouelasti and Bennacer [119] numerically studied and compared the heat transfer performances of three nano-fluids in natural convection in a differentially heated square cavity. They reported that Cu nano-particles granted best results than Al_2O_3 and TiO_2 nano-particles. Hwang et al. [120] theoretically investigated the thermal characteristics of natural convection in a

rectangular cavity heated from below with water-based nano-fluids containing alumina (Al_2O_3). Furthermore they studied the influences of the volume fraction, the size of nano-fluid and the average temperature on the heat transfer performance. They reported that as the volume fraction the of nano-particles increased, the size of the nano-particles decreased, the average temperature of nano-fluids increased and the ratio of the heat transfer coefficient of nano-fluids to that of base fluid decreased.

In 2003 Putra et al. [121] took into consideration suspensions of nano-particles of Al_2O_3 and CuO into water. They reported a systematic and definite deterioration in natural convective heat transfer. This deterioration was not present in case of conduction or forced convection. In another study the convective performances of nano-fluids have been even tested on an electronic heat sink by using CuO/water nano-fluids to actively cool down an aluminium block heated by a 150 W-cartridge heater: a maximum increase of 29.63% in convective heat transfer was achieved for a nano-fluid with a volume fraction of 0.2% compared to deionised water at a fixed volume flow rate [122].

In 2009 Nieto de Castro's group presented the concept of *ionanofluids* [123]: these are a specific type of nano-fluids made of nanomaterials suspended in ionic liquids. Ionic fluids have good heat transport and storage capabilities and very good solvent properties. In 2010 the same group [124] obtained an increase in the thermal conductivity ranging between 2% and 9%, with a weak dependence on temperature by comparing several ionic fluids with a 0.01 mass fraction of suspended MWCNTs. An enhancement of up to 8% was even found in heat thermal capacity for $[C_4mim][PF6]$ with both 0.01 and 0.015 mass fraction MWCNTs. In 2012 Nieto de Castro's group investigated the effect of temperature and concentration of MWCNT on the effective thermal conductivity and specific heat capacity of several ionanofluids. They demonstrated that the higher the concentration of MWCNTs, the higher the increase in thermal conductivity, while the temperature effect seems to be negligible.

4.6.1. Nano-fluid fabrication

The preparation of nano-fluids requires a correct dispersion of nano-particles. Two methods are commonly used to produce nano-fluids: a one-step method and a two-step method. According to Yu and Xie [126] the two-step method is the most widely used method in nano-fluids preparation. In this method, the nano-particles production and dispersion are two different operations. Firstly nano-particles are produced as dry powder. Then they are dispersed in the fluid. Two-step method is quite a cheap process, because nano-particles are already produced by several companies and are commercially available. The main problem in this procedure is the low-stability of the synthesised nano-fluid.

On the other hand, the one-step process consists of simultaneously making and dispersing the particles in the fluid. This process leads to the production of high-stability and uniform nano-fluid. According to Li et al. [117] only low vapor pressure fluids can be used in this process. This limits the application of the one-step method. In addition, other techniques, such as a continuous-flow micro-fluidic micro-reactor for Cu nano-fluid developed by Wei and Wang [127], have been developed [126], but they are not as popular as one-step and two step methods.

4.6.2. Carbon nano-tubes based nano-fluids

Use of CNT as particles for nano-fluids is found to be very effective in order to obtain fluids with high thermal conductivity. Amrollahi et al. [60] measured an enhancement of 20% by adding a 2.5 vol% of CNTs to ethylene glycol in thermal conductivity and demonstrated that traditional macro-suspensions models, such as the Maxwell and Hamilton–Crosser ones, cannot foresee the behaviour of CNT nano-fluids. In 2008 Venkata Satry et al. [61] presented a new model to predict the heat transfer in nano-fluids. In particular, they investigated the formation of extensive three-dimensional CNT chains in the liquid. They discovered that it depends on the CNT length, the volume fraction, the thermal conductivity of the base liquid, and the technique deployed to prepare the nano-fluid. Finally, the authors suggested the introduction of a new dimensionless number, termed as $\prod$, which represents the ratio of thermal resistance of the liquid to that of the CNT chains and that is able to characterise the thermal conductivity of the MWCNT nano-fluid suspension within an accuracy of $\pm 5\%$. With a 1 vol% MWCNT loading, the thermal conductivity f poly (a-olefin) oil was enhanced by more than 150% [62], water by 40% [63], and ethylene glycol by 30% [64]. In another study Kumaresan et al. [65] reported the increase in thermal conductivity and heat transfer co-efficient of CNT based nano-fluids to optimise the ratio of the CNT in nano-fluids. They suspended MWCNTs in a mixture of 70 vol% de-ionised water and 30 vol% ethylene glycol, obtaining the higher enhancements in performances with a concentration of CNT in the base liquid of 0.45 vol%. An enhancement of 19.73% and 159.3% in thermal conductivity and average heat transfer coefficient respectively were reported. The same group of researchers [66] demonstrated that 0.45 vol% of CNT is the optimal concentration when using ethylene glycol as the base liquid. The other thermo-physical properties of the nano-fluids were also found to be changed, such as the density increases with the MWCNTs concentration, while the specific heat decreases with an increase in the MWCNTs concentration. Carbon nano-tubes based nano-fluids have been used both in micro-heat pipe and in thermosyphon. In spite of enhanced thermal conductivity of the CNT based nano-fluids, the stability and life time is a major concern.

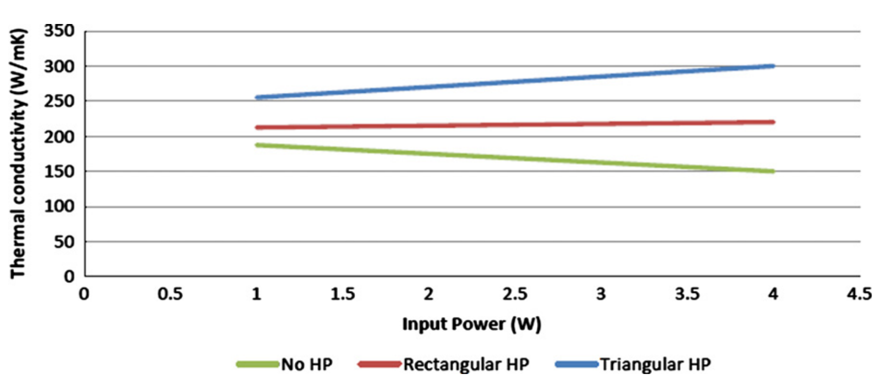


Fig. 8. Thermal conductivities of different heat pipes. Thermal conductivities of a silicon wafer with a rectangular heat pipe array, with a triangular heat pipe array and without heat pipe array, adapted by Peterson et al. [131].

Nasiri et al. [67] carried out an investigation on the stability of CNT based nano-fluids by comparing the performances of SWNTs, DWNTs, FWNTs and MWNTs suspended in water. While all the suspensions were found to be stable for months, SWNT suspension demonstrated the best stability and the higher improvements in thermal conductivity. The thermal conductivity of all suspensions decreased with time due to agglomeration. Similarly, also the reduction rates of thermal conductivity decreased with the time. However researcher reported an enhancement in thermal conductivity with the increase in temperature. To attain a better stability Meibodi et al. [68] reported optimum conditions for CNT/water nano-fluids production and operation. However it was mentioned that the more stable nano-fluids do not necessarily have the higher enhancement in thermal conductivity.

Several reviews underlined the lack of agreements among the data [116,118,125]. Some papers showed that more stable fluids are not necessarily best performing [68,125]. More works are needed on nano-fluids and standardisation in measurement procedures should be necessary for avoiding discrepancies in data. Nano-fluids have certainly shown their potential as heat transfer solution and they seem to be promising solution for devices requiring high heat removal power. Nevertheless, further investigations are required on natural convection of nano-fluids in particular. The application of CNTs in nano-fluids has shown interesting results. Finally, the development of a design able to fit the requirements of a tracked CPV system is needed.

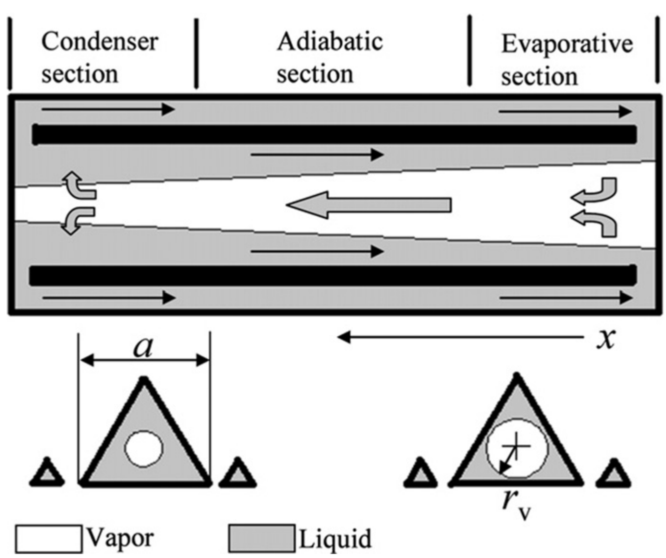


Fig. 9. MHP with arteries. Working principle of MHP with arteries [137].

4.7. Micro-heat pipes (MHP)

Heat pipes are heat exchangers which allow passively removing the heat flux from the CPV cell. Integration of a MHP can provide a better transfer of heat flux dissipated by the components to a cooler and then reduce the thermal resistance between the component and the cooler. Cotter [128] defined micro-heat pipe as “one so small that the mean curvature of the vapour–liquid interface is necessarily comparable in magnitude to the reciprocal of the hydraulic radius of the total flow channel”. In scientific literature findings both active and passive micro-heat pipes are possible. This paper focuses only on the passive cooling.

In 2007 Sobhan et al. [129] published a review of the investigations on micro-heat pipes. Yeom and Shannon [10] summarised the efforts on MHPs from 1996 to 2007. They reported that heat removed by the MHPs ranges from a few to over 300 W/cm^2. Thanks to these values, they are a feasible solution for passive CPV cooling.

4.7.1. Cross sections

As reported by Hung and Seng [130], the thermal performances of micro-heat pipe is intimately related to the cross-sectional geometry. Different cross sections are designed in order to enhance the backflow of working liquid.

As shown in Fig. 8, in 1993 Peterson et al. [131] demonstrated that the performance of a triangular micro-heat pipe is better than that of the rectangular one, due to the higher capillary pumping effect obtained in this case. Moon et al. [132] confirmed this result, using MHP with curved sections. Suman and Kumar [133] developed an analytical model to study MHP performances. They considered MHPs with two different cross sections: an equilateral triangular heat pipe with side equal to 400 μm and a rectangular (400 μm by 800 μm) heat pipe. Pentane was the working fluid with silicon as the substrate. Suman and Kumar [133] demonstrated that the performance of a heat pipe goes down with the increase in the number of sides.

Kang and Huang [134] fabricated a star grooved MHP and a rhombus grooved MHP. They reported an increase in thermal conductivity of 33.6% for the star grooved MHP and of 39.1% for the rhombus grooved MHP when compared with a traditional triangular MHP. The authors stated that the better capillarity was provided by more acute angles and micro-gaps in the star- and rhombus-groove devices.

As reported by Hung and Seng [130], the acuteness and the number of sharp corners are two important basic geometrical factors that govern the capillarity pumping ability and hence the performance of a micro-heat pipe. For regular polygonal shapes, the acuteness of the corner and the number of corners are dependent: the corner apex angle decreases when the number of corners increases. In star-grooved MHP number of corners and corner apex

Table 4
Nano-fluids in micro-grooved heat pipes publications, adapted by Lio and Li [139]

Shape of micro-grooved heat pipe	Best performing working liquid type (nanoparticle size and optimal concentration)	Maximum reduction in thermal resistance (fluid compared with)	Researchers
Disk-shaped	Au/Water (17 nm)	Average of 40% (DI water)	Chien et al. [138]
Cylindrical	Ag/Water (10 nm)	50% (water)	Kang et al. [140]
Cylindrical	Ag/Water (35 nm)	80% (water)	Kang et al. [140]
Cylindrical	Ag/Water (10 nm)	44% (water)	Wei et al.
Cylindrical	CuO–water (50 nm, 1.0 wt%)	39% (water)	Yang et al. [141]
Flat	Al_2O_3–water (38.4 nm, 0.8 wt%)	47.7% (DI water)	Do K.H. and Jang S.P. [142]
Flat-shape	TiO_2–water (20 nm, 4.0 wt%)	27% (water)	Shafahi et al. [143]
Cylindrical	TiO_2–water (10 nm, 4.0 wt%)	25% (water)	Shafahi et al. [144]
Cylindrical	CuO–water (50 nm, 1.0 wt%)	About 50% (water)	Liu et al. [145]
Cylindrical	CuO–water (50 nm, 1.0 wt%)	50% (water)	Wang et al. [146]

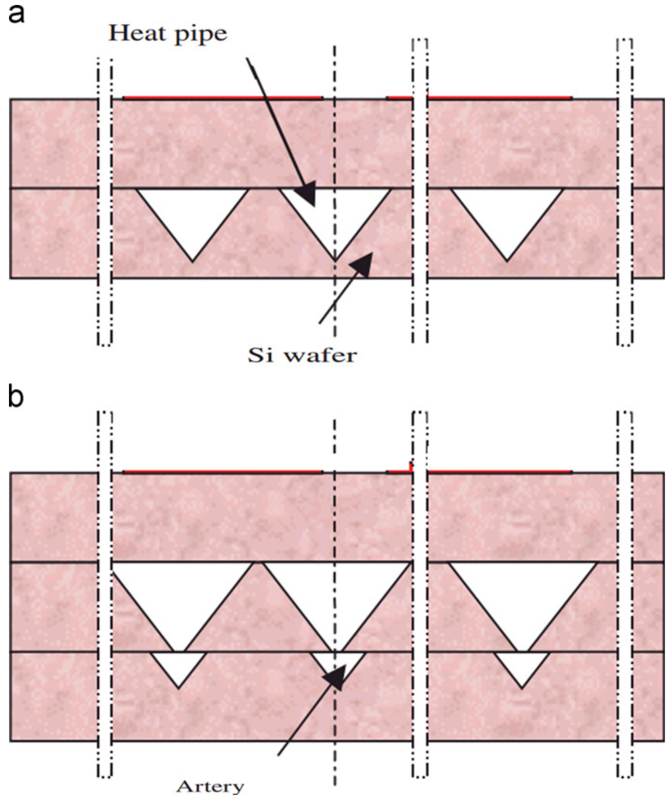


Fig. 10. Cross-section of a MHP. Transverse cross-sections of a Le Berre et al. [148] MHP.

angles do not affect each other. For these reasons Hung and Seng [130] stated that star-groove micro-heat pipes render higher capillary pumping power and hence higher heat transport capacity compared to those of regular polygonal micro-heat pipes. Furthermore, they discovered that the increase in the total length of the micro-heat pipe results in decrease of its heat transport capacity.

In a review, Sobhan et al. [129] reported an innovative design: a wire bonded MHP. Wang and Peterson [135] proposed a wire-bonded micro-heat pipe array. The authors investigated the performance of wire-bonded aluminium–acetone micro-heat pipe both analytically and experimentally. The MHP was obtained by sandwiching an array of cylindrical wires between two flat plates. They discovered that the maximum heat transfer capacity increased with the increase in both wire diameter and operating temperature to a maximum value and then decreases within the operating temperature range of the working fluid. Moreover they demonstrated that increasing the spacing between wires can increase the maximum heat transport capacity. In their following work, Wang and Peterson [136] confirmed this statement, but added that there is a spacing value where this improvement is overshadowed by the decrease in the number of heat pipes in the

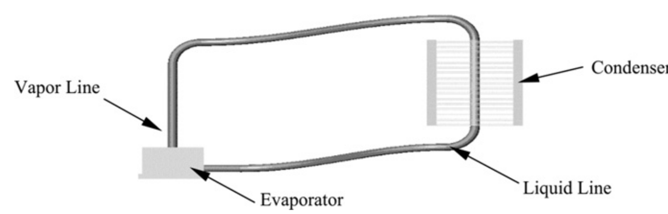


Fig. 12. Loop thermosyphon. Conceptual design of the loop thermosyphon [150].

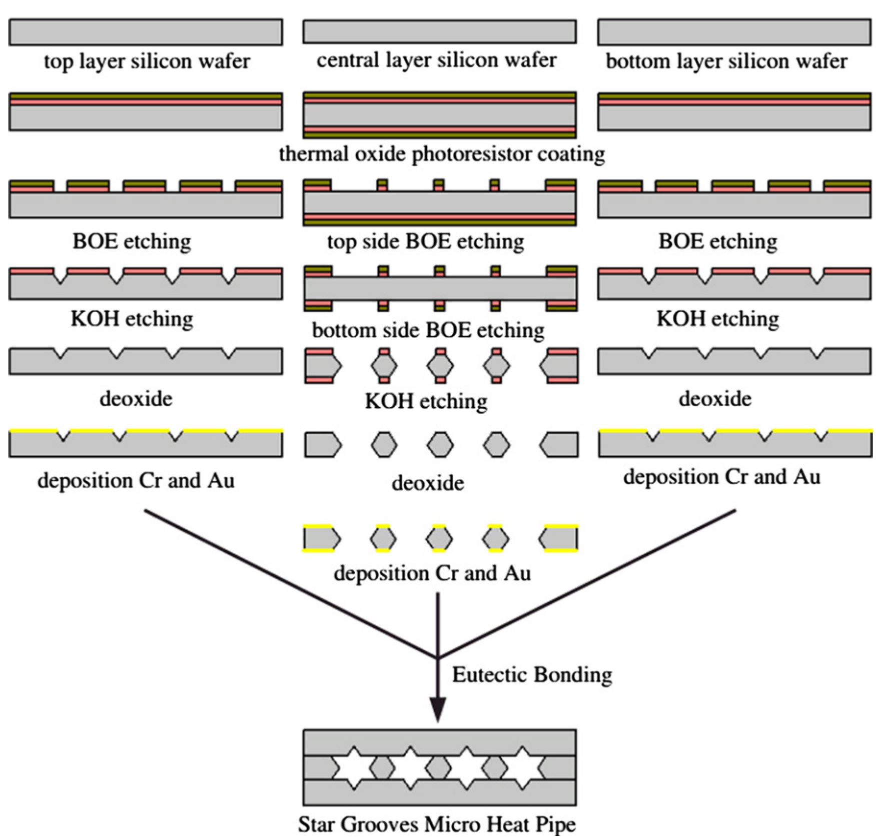


Fig. 11. Star grooved MHP machining. Fabrication process of the star grooved MHP [134].

Table 5
Comparison of different micro- and nano-technologies.

Cooling technologies	Manufacturability	Applied to CPV	References	Remarks
Heat spreaders	Chemical vapour deposition	N.A.*	[28,30,33]	Mature technology, able to assure extremely high thermal conductivity.
Natural convection in micro-channels	Wet etching; dry etching	Only as active cooling	[38–40]	Further investigations on material specifications are required.
Carbon nano-tubes	Arc discharge; chemical vapour deposition; laser ablation	N.A.	[20,48,53]	Highest heat transfer performances among reported technologies. Material stability is an issue that need to be addressed.
Micro-fins	Dry etching (DRIE, RIE)	Yes	[94,98,99]	Simple solution, suitable for low concentration CPV
Nano-wires		N.A.	[107–109]	Not suitable for passive cooling, due to low thermal conductivity.
Natural convection of nano-fluids	One-step method; two-step method.	N.A.	[113,116,126]	Further investigations are required. Suitable for active cooling.
Micro-heat pipes	Standard etching technologies	N.A.	[129,134,147]	High heat removing capacity. Suitable for passive CPV cooling.
Miniature thermosyphons	Standard micro-fabrication techniques	N.A.	[24,149,153]	Not suitable for orientation-dependent applications.

* N.A.: Not Available.

array, and the maximum heat transfer capacity becomes limited. The optimum spacing distance varies with the diameter.

4.7.1.1. MHP with arteries. This design consists of one vein channel which is the traditional MHP and two neighbour arterial channels distributed on both sides of the vein and connected together at both ends (Fig. 9). In the vein, vapour carries the latent heat flowing to the cold end where it condenses. In the arteries, the liquid is transported to the hot end by the capillary force applied by the V-grooves in the micro-triangle pipes. Thanks to the liquid pressure difference between the cold end of artery and MHP, the liquid gathered at the condenser section can be transported back.

Liu et al. [137] compared two kinds of MHP: with and without arteries. At the end of their research, the authors stated that implanted arteries can effectively enhance the capillary force thus improving the capability to transport the liquid from the cold end back to the hot end, and limiting the propagation of dry-out region.

4.7.2. Working fluids

The working fluid is an important aspect for the efficiency of micro-heat pipes, which are the two-phase cooling devices. In 2003 Chien et al. [138] proposed the use of nano-fluids into the micro-heat pipes. Using nano-gold particles suspended in water, instead of pure water, the authors obtained an average decrease of 40% in the MHP thermal resistance. Over 30 papers on the application of nano-fluids into heat pipes have been published so far [139]. For the purposes of this review, just the works on micro-grooved heat pipes have been considered. A summary of the results is reported in Table 4: each research shows an enhancement in MHP thermal exchange due to the use of nano-fluids. Liu and Li [139] reported three main reasons for these enhancements in thermal transfer: the effective thermal conductivity of nano-fluids increases; the physical properties of nano-fluids change, increasing the capillary force in the HP and making the liquid to extend in the micro-grooves; nano-particles form a thin porus layer on the wall, which increases the capillary force.

4.7.3. MHP fabrication

Micro-heat pipes fabrication usually involves standard micro-systems technologies. Ivanova et al. [147] fabricated a silicon/water MHP using two silicon wafers. Deep plasma etching was used to obtain the micro-capillary wick. On one wafer, small diameter holes were laser-drilled for filling. The two wafers are assembled by Silicon Direct Bonding technique. Finally a thermal annealing under inert gas then leads to irreversible bonding due to the formation of covalent bonds between the two surfaces

In 2002 Le Berre et al. [148] fabricated and tested two types of silicon micro-heat pipes. The first one (shown in Fig. 10a) consisted of a series of 55 parallel triangular shaped channels, 230 μm wide, 170 μm deep, 20 mm long and with a spacing of 130 μm that are micro-machined into a silicon wafer. A second wafer is then sealed to the first one to hermetically close the device. For the second design (Fig. 10b), arteries are added for the liquid transport: the liquid returns via independently etched channels to the evaporator. In this case, the first wafer consists of 25 triangular grooves, 500 μm wide, 320 μm deep, etched throughout the wafer. The second wafer contains 25 triangular grooves too. The fabrication started with the thermal growth of a 1.5 μm oxide layer on the device wafer. The oxide on both sides of the device wafer is patterned in order to be used as an etching mask. Triangular grooves are etched using a 40 wt% aqueous KOH solution at 60-C. Plain silicon wafers were used to seal the MHP arrays (*Si–Si direct bonding*).

Kang and Huang [134] fabricated a star grooves MHP formed by three (100) silicon wafers. They used photolithography wet etching technology, to etch a series of 31 parallel V-grooves. Then the three layers of the wafers were eutectic bonded to form the MHP. All these processes are presented in Fig. 11.

4.8. Miniature two phase closed thermosyphon

Two phase closed thermosyphons are also known as *wickless heat pipe* (Fig. 12). Lee [149] defined them as the heat pipes which do not use the capillary force. Thermosyphons exploit gravitational laws: so, they cannot be used in special or for orientation-dependent applications. Thus, they cannot be easily applied to a CPV, which usually requires a tracking system.

Wickless micro-heat pipe was conceived first in 1984, by Cotter [128]. He investigated a cooling system "for applications calling for close temperature control, but having only modest cooling requirements". In 1998, Gromoll [24] stated that thermosyphons can be used for power loss densities up to 30 W/cm^2: at higher temperatures film boiling begins, decreasing cooling efficiency. On the other hand, in 2007, Yeom and Shannon [10] reported a maximum heat flux of 200 W/cm^2.

Pal et al. [150] tested two working fluids on a compact thermosyphon for PC cooling: deionized ultrafiltered water and PF5060, a dielectric liquid. They stated that water was a better working fluid, because of its better thermal properties than those of PF5060. However, they proposed the exploitation of a proper degassing procedure to improve the performance of the PF5060

charged system. Several works have been published on the exploitation of nano-fluids in closed two-phase thermosyphons [139], but only few of them focus on miniature thermosyphons and are reported in this work. Presenting the considerations of Liu and Li [139] about the realiability of nano-fluids in thermosyphons is interesting for the aims of this review. The authors realized that the nanoparticles generally proved to be able to increase the heat transfer in the majority of the experiments, but those few works reported the opposite results. This discrepancy should depend on several factors: the porus sediment in the boiling process, the impact of the operating temperature on the thermal performance, the preparation of the nano-fluids. The same group [151,152] carried out two experiments to discover the performance of an active miniature thermosyphon using a water–CuO nano-fluid or a carbon nano-tube based nano-fluid. Firstly they demonstrated that the heat transfer performance of the miniature thermosyphon can evidently be strengthened by using water–CuO nano-fluid [151]. In the second work [152], the researchers obtained a lower thermal resistance and a more uniform temperature distribution in the micro-thermosyphon using carbon nano-tube suspension instead of deionized water. Furthermore they stated that mass concentration of 2.0% corresponds to the optimal heat transfer enhancement.

Ramaswamy et al. [153] investigated the effect of channel width on the miniature thermosyphon performances. The authors discovered an increase in heat dissipation when increasing the pore size.

4.8.1. *Thermosyphon fabrication*

Ramaswamy et al. [153] tested several micro-fabrication techniques to fabricate a silicon thermosyphon. Wafer dicing, laser milling and wet etching were used to etch the channels into the silicon wafer. According to them, wet etching seemed to be the most promising method for bulk fabrication and resulted in very clean channels. Furthermore several bonding techniques were tried, including direct wafer bonding, eutectic bonding, and epoxy bonding. The authors stated that very good bonding was attained with an aluminium–silicon eutectic and cyanate ester epoxy.

5. Conclusions

This review investigated micro-and nano-technologies which could be used for passive CPV cooling. The fabrication processes have also been covered. Among the reported solutions, carbon nano-tubes seem to be able to offer the best cooling performances, as described in Table 5.

A lot of researches were carried out on CNTs in the last two decades, due to their important thermal and mechanical properties. High thermal conductance and high performance improvements have been demonstrated in several papers using carbon nano-tubes. CNTs fabrication processes are mature techniques: several synthesising methods have been developed and tested. High-purity carbon nano-tubes have been obtained by different groups without the application of a purification process.

Another promising and simple technology is the high-conductive coating. A diamond layer can be fabricated through a well-known chemical vapour deposition process. However to overcome the high costs and, at the same time, to maintain high performances, the exploitation of composite materials has to be taken into account. Micro-heat pipes and micro-fins can also be considered as plausible solutions for passive CPV cooling. Further investigations are required on nano-fluid in natural convection to understand the real potentials of these solutions.

Only in a few cases, micro- and nano-technologies were applied to concentrating photovoltaic systems. More experimental researches are needed to investigate the applicability and the performances of these technologies to CPV, but the present comparisons may provide a good background.

Acknowledgement

This work was financially supported by EPSRC-DST funded BioCPV project. The authors wish to thank Dr. Prabhakara Bobbili for his help in thermosyphons and heat pipes exploration.

References

[1] Kurtz S. Opportunities and challenges for development of a mature concentrating photovoltaic power industry; 2009.
[2] Royne A, Dey C, Mills D. Solar Energy Materials and Solar Cells 2005;86:451–83.
[3] Friedman DJ. Current Opinion in Solid State and Materials Science 2010;14:131–8.
[4] Green MA, Emery K, Hishikawa Y, Warta W, Dunlop ED.; 2012. p. 12–20.
[5] Slade A, Garboushian V. Technical digest, 15th international; 2005. p. 1–2.
[6] Philipps SP, Dimroth F, Bett AW. Practical handbook of photovoltaics. Elsevier Ltd; 2012 p. 417–48.
[7] Martinelli G, Stefancich M. Concentrator photovoltaics. Springer; 2007 p. 133–49.
[8] Zhangbo Y, Qifen L, Qunzhi Z, Weiguo P. IEEE 6th international power electronics and motion control conference, vol. 3; 2009. p. 2193–7.
[9] Kinsey GS, Edmondson KM. Solar Cells 2009:279–88.
[10] Yeom J, Shannon MA. Comprehensive microsystems. New York: Elsevier; 2007 p. 499–550.
[11] Tseng Y-S, Fu H-H, Hung T-C, Pei B-S. Applied Thermal Engineering 2007;27:1823–31.
[12] Anderson WG, Tamanna S, Sarraf DB, Dussinger PM, Hoffman RW Jr. Heat pipe cooling of Concentrating Photovoltaic (CPV) systems; n.d.
[13] Liu L, Zhu L, Wang Y, Huang Q, Sun Y, Yin Z. Solar Energy 2011;85:922–30.
[14] Han X, Everett V, Wang Y, Zhu L. Japanese Journal of Applied Physics 2009:2009.
[15] Zhu L, Boehm RF, Wang Y, Halford C, Sun Y. Solar Energy Materials and Solar Cells 2011;95:538–45.
[16] Zhu L, Boehm RF, Wang Y, Halford C, Sun Y. Solar Energy Materials and Solar Cells 2011;95:538–45.
[17] Mokri A, Emziane M. In: Moshfegh B (editor). World Renewable Energy Congress—Sweden. Linköping, Sweden, Linköping; 8–13 May, 2011. p. 2738–42.
[18] Gombert A. S.S. Gmbh, B. Street; 2011. p. 1651–56.
[19] Extance A, Marquez C. CPV Today 2010.
[20] Shakouri BA. Nanotechnology 2006;94:1613–38.
[21] Bhushan B. Seminars in Cell Developmental Biology 2010;714:1–6.
[22] Müller M, Escher W, Ghannam R, Goicochea J, Michel B, Ong CL, et al. AIP Conference Proceedings 2011:231–4.
[23] Gururatana S. American Journal of Applied Sciences 2012;9:436–9.
[24] Gromoll B. Revue Générale De Thermique 1998;37:781–7.
[25] Cahill DG, Ford WK, Goodson KE, Mahan GD, Majumdar A, Maris HJ, et al. Journal of Applied Physics 2003;93:793–818.
[26] Gates BD, Xu Q, Love JC, Wolfe DB, Whitesides GM. Annual Review of Materials Research 2004;34:339–72.
[27] Qin D, Riggs BA. Encyclopedia of supramolecular chemistry. Taylor & Francis; 2012 p. 1–9.
[28] Jagannadham K, Watkins T, Dinwiddie R. Journal of Materials Science 2002;37:1363–76.
[29] Abyzov AM, Kidalov SV, Shakhov FM. Applied Thermal Engineering 2012;48:72–80.
[30] Bar-cohen A, Wang P. Nano-bio-electronic, photonic and MEMS packaging. In: Wong CP, Moon K-S, (Grace) Li Y, editors. US, Boston, MA: Springer; 2010 p. 349–429.
[31] Gray KJ. Diamond and Related Materials 2000;9:201–4.
[32] Zhang Z, Schneider H, Tounsi P. Materials Science and Engineering: B 2012;177:1358–61.
[33] Twitchen DJ, Pickles CSJ, Coe SE, Sussmann RS, Hall CE. Diamond and Related Materials 2001;10:731–5.
[34] Sung JC, Kan M-C, Hu S-C, Sung M, Montheith BG, 〈http://www.advanceddiamond.com/whitepapers/DiamondCompositeHeatSpreader.pdf〉.
[35] Nishiyabu K, Kanoko Y, Tanabe D, Tanaka S. Metal Powder Report 2011;66:27–32.
[36] Chein R, Chuang J. International Journal of Thermal Sciences 2007;46:57–66.
[37] Guo Z-Y, Li Z-X. International Journal of Heat and Fluid Flow 2003;24:284–98.
[38] Buonomo B, Manca O. International Journal of Thermal Sciences 2012:1–13.
[39] Chen C-K, Weng HC. Journal of Heat Transfer 2005;127:1053.

[40] Buonomo B, Manca O. International Journal of Thermal Sciences 2010;49:1333–44.
[41] Haddad OM, Abuzaid MM, Al-Nimr MA. Numerical Heat Transfer, Part A: Applications 2005;48:693–710.
[42] Tjerkstra RW, De Boer M, Berenschot E, Gardeniers JGE, van den Berg A, Elwenspoek MT. An investigation of micro-structures, sensors, actuators, machines and robots. In: Proceedings of the IEEE tenth annual international workshop on micro-electro mechanical systems ; 1997. p. 147–52.
[43] Dwivedi VK, Gopal R, Ahmad S. Microelectronics Journal 2000;31:405–10.
[44] Alavi M, Büttgenbach S, Schumacher A, Weingarten H-J. Sensors and Actuators A: Physical 1992;32:299–302.
[45] Kam DH, Shah L, Mazumder J. Journal of Micromechanics and Microengineering 2011;21:045027.
[46] Chen T, Si J, Hou X, Kanehira S, Miura K, Hirao K. Applied Physics Letters 2008;93:051112.
[47] Iijima S. Nature 1991;354:56–8.
[48] Aqel A, El-Nour KMMA, Ammar RAA, Al-Warthan A. Arabian Journal of Chemistry 2010;5:1–23.
[49] Reilly RM. Journal of Nuclear Medicine: Official Publication, Society of Nuclear Medicine 2007;48:1039–42.
[50] Ying LS, bin Mohd Salleh MA, Mohamed Yusoff HB, Abdul Rashid SB, Abd. Razak JB. Journal of Industrial and Engineering Chemistry 2011;17:367–76.
[51] Qian C, Qi H, Gao B, Cheng Y, Qiu Q, Qin L-C, et al. Journal of Nanoscience and Nanotechnology 2006;6:1346–9.
[52] Endo M, Strano MS, Ajayan PM. Carbon Nanotubes 2008;62:13–62.
[53] Han Z, Fina A. Progress in Polymer Science 2011;36:914–44.
[54] Chiavazzo E, Asinari P. Nanoscale Research Letters 2011;6:249.
[55] Kim P, Shi L, Majumdar A, McEuen P. Physical Review Letters 2001;87: 19–22.
[56] Jakubinek MB, White MA, Li G, Jayasinghe C, Cho W, Schulz MJ, et al. Carbon 2010;48:3947–52.
[57] Tong T, Zhao Y, Delzeit L, Kashani A, Meyyappan M, Majumdar A. Packaging 2007;30:92–100 (Boston, Mass).
[58] Berber S, Kwon Y, Tomanek D. Physical Review Letters 2000;84:4613–6.
[59] Korda´s K, To´th G, Moilanen P, Kumpumäki M, Vähäkangas J, Uusimäki a, et al. Applied Physics Letters 2007;90:123105.
[60] Amrollahi a, Hamidi AA, Rashidi AM. Nanotechnology 2008;19:315701.
[61] Venkata Sastry NN, Bhunia A, Sundararajan T, Das SK. Nanotechnology 2008;19:055704.
[62] Choi SUS, Zhang ZG, Yu W, Lockwood FE, Grulke EA. Applied Physics Letters 2001;79:2252.
[63] Assael MJ, Chen C-F, Metaxa I, Wakeham WA. International Journal of Thermophysics 2004;25:971–85.
[64] Hwang Y, Ahn Y, Shin H, Lee C, Kim G, Park H, et al. Current Applied Physics 2006;6:1068–71.
[65] Kumaresan V, Velraj R, Das SK. International Journal of Refrigeration 2012:1–10.
[66] Kumaresan V, Velraj R. Thermochimica Acta 2012;545:180–6.
[67] Nasiri a, Shariaty-Niasar M, Rashidi AM, Khodafarin R. International Journal of Heat and Mass Transfer 2012;55:1529–35.
[68] Meibodi ME, Vafaie-Sefti M, Rashidi AM, Amrollahi A, Tabasi M, Kalal HS. International Communications in Heat and Mass Transfer 2010;37:319–23.
[69] Keidar M. Journal of Physics D: Applied Physics 2007;40:2388–93.
[70] Engel-Herbert R, Pforte H, Hesjedal T. Materials Letters 2007;61:2589–93.
[71] Takagi D, Homma Y, Kobayashi Y. Physica E: Low-Dimensional Systems and Nanostructures 2004;24:1–5.
[72] Gore JP, Sane A. Carbon nanotubes—synthesis, characterization, applications. In: Yellampalli S, editor. InTech; 2011.
[73] Maser WK, Benito AM, Martınez MT. Source 2002;40:1685–95.
[74] Nikolaev P, Bronikowski M, Bradley RK, Rohmund F, Colbert DT, Smith KA, et al. Chemical Physics Letters 1999:91–7.
[75] See CH, Harris AT. Industrial and Engineering Chemistry Research 2007;46:997–1012.
[76] Isaacs JA, Tanwani A, Healy ML, Dahlben LJ. Journal of Nanoparticle Research 2009;12:551–62.
[77] Jašek O, Eliáš M, Zajíčková L, Kudrle V, Bublan M, Matějková J, et al. Materials Science and Engineering: C 2006;26:1189–93.
[78] Jašek O, Eliáš M, Zajíčková L, Kucerova Z, Matejkova J, Rek A, et al. Journal of Physics and Chemistry of Solids 2007;68:738–43.
[79] Zajíčková L, Synek P, Jašek O, Eliáš M, David B, Buršík J, et al. Applied Surface Science 2009;255:5421–4.
[80] Schwandt C, Dimitrov AT, Fray DJ. Carbon 2012;50:1311–5.
[81] Diener MD, Nichelson N, Alford JM. Society 2000:9615–20.
[82] Height MJ, Howard JB, Tester JW. Proceedings of the Combustion Institute 2005;30:2537–43.
[83] Naha S, Sen S, De AK, Puri IK. Proceedings of the Combustion Institute 2007;31:1821–9.
[84] Smith MR, Hedges SW, Lacount R, Kern D, Shah N, Huffman GP, et al. Carbon 2003;41:1221–30.
[85] Rosca I, Watari F, Uo M, Akasaka T. Carbon 2005;43:3124–31.
[86] Suri A, Coleman KS. Carbon 2011;49:3031–8.
[87] MacKenzie K, Dunens O, Harris AT. Separation and Purification Technology 2009;66:209–22.
[88] Shelimov KB, Esenaliev RO, Rinzler AG, Huffman CB, Smalley RE. Scanning 1998:429–34.
[89] Vaccarini L, Goze C, Aznar R, Micholet V, Journet C, Bernier P, et al. Comptes Rendus De l'Académie Des Sciences-Series IIB-Mechanics-Physics-Astronomy 1999;327:925–31.
[90] Hong KB, Ismail AAB, Mahayuddin MEBM, Mohamed AR, Zein SHS. Journal of Natural Gas Chemistry 2006;15:266–70.
[91] Dasgupta K, Venugopalan R, Sathiyamoorthy D. Materials Letters 2007;61: 4496–4499.
[92] Fleury D, Bomfim JAS, Vignes A, Girard C, Metz S, Muñoz F, et al. Journal of Cleaner Production 2011.
[93] Ok ZD, Benneyan, JC, Isaacs JA. In: Proceedings of the 2007 IEEE international symposium on electronics and the environment; 2007 p. 85–90.
[94] Natarajan SK, Mallick TK, Katz M, Weingaertner S. International Journal of Thermal Sciences 2011;50:2514–21.
[95] Do KH, Kim TH, Han Y-S, Choi B-I, Kim M-B. Solar Energy 2012;86:2725–34.
[96] Mittelman G, Dayan A, Dado-Turjeman K, Ullmann A. International Journal of Heat and Mass Transfer 2007;50:2582–9.
[97] Kim JS, Park BK, Lee JS. Experimental Heat Transfer 2008;21:55–72.
[98] Mahmoud S, Al-Dadah R, Aspinwall DK, Soo SL, Hemida H. Applied Thermal Engineering 2011;31:627–33.
[99] Shokouhmand H, Ahmadpour A. In: Proceedings of the world congress on engineering; 2010.
[100] Laermer F, Schilp A. US Patent 6284148; 2001.
[101] Peles Y, Koşar A, Mishra C, Kuo C-J, Schneider B. International Journal of Heat and Mass Transfer 2005;48:3615–27.
[102] Bopp M, Coronel P, Hibert C, Ionescu AM. Microelectronic Engineering 2010;87:1348–51.
[103] Laermer F, Franssila S, Sainiemi L, Kolari K. In: Veikko L, Markku T, Ari L, Teruaki M, editors. Handbook of silicon based MEMS materials and technologies. Elsevier; 2009 p. 349.
[104] Murakami K, Wakabayashi Y, Minami K, Esashi M. Micro-electro mechanical systems, MEMS'93. In: IEEE Proceedings of an investigation of micro-structures, sensors, actuators, machines and systems; 1993. p. 65–70.
[105] Kosar A, Mishra C, Peles Y. Journal of Fluids Engineering 2005;127:419.
[106] Abdolvand R, Ayazi F. Sensors and Actuators A: Physical 2008;144:109–16.
[107] Zhang G. Nanowires—fundamental research. In: Hashim A, editor. InTech; 2008.
[108] Li J, Yu H, Wong SM, Li X, Zhang G, Lo PG-Q, et al. Applied Physics Letters 2009;95:243113.
[109] Jet Propulsion Laboratory. NASA Tech Briefs; 2007. p. 42–3.
[110] Volz SG, Chen G. Applied Physics Letters 1999;75:2056.
[111] Li Y, Buddharaju K, Singh N, Lo GQ, Lee SJ. Power 2010:1181–5.
[112] Masuda H, Ebata A, Teramae K, Hishinuma N. Netsu Bussei 1993;7:227–33.
[113] Choi SUS, Eastman JA. ASME-Publications-FED, vol. 231; 1995. p. 99–106.
[114] Rafati M, Hamidi AA, Shariati Niaser M. Applied Thermal Engineering 2012;45–46:9–14.
[115] Wong KV, De Leon O. Advances in Mechanical Engineering 2010;2010:1–11.
[116] Godson L, Raja B, Mohan Lal D, Wongwises S. Renewable and Sustainable Energy Reviews 2010;14:629–41.
[117] Li Y, Zhou J, Tung S, Schneider E, Xi S. Powder Technology 2009;196:89–101.
[118] Kleinstreuer C, Feng Y. Nanoscale Research Letters 2011;6:229.
[119] Oueslati FS, Bennacer R. Nanoscale Research Letters 2011;6:222.
[120] Hwang K, Lee J, Jang S. International Journal of Heat and Mass Transfer 2007;50:4003–10.
[121] Putra N, Roetzel W, Das SK. Heat and Mass Transfer 2003;39:775–84.
[122] Selvakumar P, Suresh S. Experimental Thermal and Fluid Science 2012;40:57–63.
[123] Nieto de Castro CA, Murshed SMS, Lourenço MJV, Santos FJV, Lopes MLM, França JMP. International Journal of Thermal Sciences 2012:6–11.
[124] Nieto de Castro CA, Lourenço MJV, Ribeiro APC, Langa E, Vieira SIC. Journal of Chemical and Engineering Data 2010;55:653–61.
[125] Ghadimi A, Saidur R, Metselaar HSC. International Journal of Heat and Mass Transfer 2011;54:4051–68.
[126] Yu W, Xie H. Journal of Nanomaterials 2012;2012:1–17.
[127] Wei X, Wang L. Particuology 2010;8:262–71.
[128] Cotter T. Principles and prospects for micro-heat pipes; 1984.
[129] Sobhan CB, Rag RL, Peterson GP. International Journal of Energy Research 2007:664–88.
[130] Hung YM, Seng Q. International Journal of Heat and Mass Transfer 2011;54:1198–209.
[131] Peterson GF, Duncan AB, Weichold MH. Journal of Heat Transfer 1993;115:751–6.
[132] Moon SH, Hwang G, Ko SC, Kim YT. Experimental study on the thermal performance of micro-heat pipe with cross-section of polygon. Microelectronics Reliability 2004;44:315–21.
[133] Suman B, Kumar P. International Journal of Heat and Mass Transfer 2005;48:4498–509.
[134] Kang S, Huang D. Sensors 2002;525 (Peterborough, NH).
[135] Wang YX, Peterson GP. Journal of Thermophysics and Heat Transfer 2002;16:346–55.
[136] Wang Y, Peterson GP. Journal of Thermophysics and Heat Transfer 2002;16:537–46.
[137] Liu W, Kang J, Fu X, Stefanini C, Dario P. Microelectronic Engineering 2011;88:2255–8.
[138] Chien H, Tsai C, Chen P, Chen P. Micro 2003:389–91.
[139] Liu Z-H, Li Y-Y. International Journal of Heat and Mass Transfer 2012;55:6786–97.

[140] Kang S-W, Wei W-C, Tsai S-H, Yang S-Y. Applied Thermal Engineering 2006;26:2377–82.
[141] Yang XF, Liu Z-H, Zhao J. Journal of Micromechanics and Microengineering 2008;18:035038.
[142] Do KH, Jang SP. International Journal of Heat and Mass Transfer 2010;53:2183–92.
[143] Shafahi M, Bianco V, Vafai K, Manca O. International Journal of Heat and Mass Transfer 2010;53:1438–45.
[144] Shafahi M, Bianco V, Vafai K, Manca O. International Journal of Heat and Mass Transfer 2010;53:376–83.
[145] Liu Z-H, Li Y-Y, Bao R. International Journal of Thermal Sciences 2010;49:1680–7.
[146] Wang G-S, Song B, Liu Z-H. Experimental Thermal and Fluid Science 2010;34:1415–21.
[147] Ivanova M, Lai A, Gillot C, Sillon N, Schaeffer C, Lefèvre F, et al. The Tenth intersociety conference on thermal and thermomechanical phenomena in electronics systems ITHERM'06; 2006. p. 545–51.
[148] Berre ML, Launay S, Sartre V, Lallemand M, Micromech J. Microengineering 2003;13:436–41.
[149] Lee Y. Applied Thermal Engineering 1996;16:655–68.
[150] Pal A, Joshi YK, Beitelmal MH, Patel CD, Wenger TM. IEEE Transactions on Components and Packaging Technologies 2002;25:601–7.
[151] Liu ZH, Yang XF, Guo GL. Journal of Applied Physics 2007;102:013526.
[152] Liu Z, Yang X, Wang G, Guo G. International Journal of Heat and Mass Transfer 2010;53:1914–20.
[153] Ramaswamy C, Joshi Y, Nakayama W, Johnson W. Microscale Thermophysical Engineering 1999;3:273–82.